Rotational seismic excitation effects on CIDH pile-supported bridge piers

Elli-Konstantina V. Mylona[1], Anastasios G. Sextos[2], George E. Mylonakis[3]

ABSTRACT

This paper investigates the response of bridges founded on single, cast-in-drilled-hole (CIDH) piles under combined translational and rotational excitation. The input motion stems from kinematic interaction - a result of the relative flexibility between pile and soil - and subsequent pile bending, under the passage of vertically propagating seismic shear waves. The rotational component of seismic excitation is typically ignored in analysis and design, and it is not prescribed in modern seismic codes. More importantly, the significance of this effect on the response of pile-supported bridges has not been quantified and is presently poorly understood. Along these lines, a simple framework is presented in this paper for studying parametrically: (a) the salient features of the rotational excitation component and (b) the seismic demand imposed on the superstructure. For this purpose, multiple MDOF oscillators representing typical bridge piers of different heights, founded on soils of different stiffness, are considered, subjected to a variety of harmonic signals and recorded earthquake motions. The displacement demands on the superstructure are compared to corresponding displacements obtained under exclusively translational excitation. It is concluded that the kinematically-induced rotational excitation may significantly increase deck displacements (by a factor of 2 or more depending on the circumstances), especially close to resonant frequencies associated with the dynamic characteristics of the soil and the superstructure.

Keywords: Rotational excitation, CIDH pile foundation, kinematic interaction, soil–structure interaction

[1] Civil Engineer, MSc., Ph.D. Candidate, Aristotle University, Thessaloniki, Greece
[2] Associate Professor, University of Bristol, U.K. and Aristotle University, Thessaloniki, Greece
Corresponding Author, e-mail: a.sextos@bristol.ac.uk, asextos@civil.auth.gr
[3] Professor, University of Bristol, U.K. and University of Patras, Greece; Adjunct Professor, University of California, Los Angeles, U.S.A. e-mail: g.mylonakis@bristol.ac.uk

1. INTRODUCTION

In the age of rapid transportation, importance of bridge safety can hardly be overstated. Following a series of catastrophic earthquakes that inflicted serious damage on bridges (San Fernando 1971, Loma Prieta 1989, Northridge 1994, Kobe 1995, Kocaelli 1999, Maule 2010, Tohoku 2011), research on earthquake performance of bridge structures has turned into a mainstream area in structural and dynamics engineering. Recent seismic codes prescribe means to ensure a target level of bridge performance related to integrity and serviceability for various levels of earthquake loading, so that the probability of massive human loss is reduced and the disruption of social and financial activity is limited to a minimum.

Despite their relatively simple structural form (compared to buildings), bridges may exhibit complex dynamic response. This stems from their large dimensions, asymmetry in plan, kinematic constraints such as stoppers and shear keys, potentially significant contribution of higher modes, sensitivity to spatially variable foundation properties and ground motion, as well as on topography and/or soft geologic formations of the areas crossed. It is, therefore, not surprising that the superstructure – foundation – subsoil system is often studied as a whole, with full consideration of the interactions among its components and the spatially variable nature of foundation conditions and earthquake input.

The inherent complexity of bridge response has been thoroughly studied in recent years, and progress on bridge research, especially in pile supported structures, has been achieved thanks to analytical solutions and advanced numerical simulations [1,2] encompassing site response [3] and soil-pile behaviour [4–7]. Experimental results involving complex bridge structures on pile foundations are also available [8–10], while theoretical research has shed light into the nature of kinematic soil-pile interaction [11–16]. Furthermore, calibrated models from experimental tests and free-field measurements on Test Sites [17,18] have demonstrated the SSI effects for a range of ground motion intensities.

A potentially important issue that has not received proper attention by researchers and code writers is the rotational excitation imposed at the base of a pile–supported bridge pier due to kinematically–induced rotation of the pile head [19,20]. This rocking differs from the ordinary rotation of the pile head developing as a result of soil-foundation compliance (modelled by the well-known foundation springs and dashpots at the pile head), as in this case the rotation is also part of the excitation – not just response. In other words, the presence of a pile foundation modifies the amplitude and frequency content of the incoming seismic waves, thus resulting to an input motion that is different from the

motion of the free field and includes the aforementioned rotational component. When the system is analysed as a whole, the rotational excitation is inherent in the response. However, in most cases sub-structuring techniques are employed, which require proper consideration of the imposed kinematic rotation. It is noted that while in surface footings development of rotational excitation requires inclined or surface seismic waves, in pile foundations this happens with vertically propagating S waves as well.

Analytical expressions have been derived for computing the kinematic pile head rotation under idealised conditions [16,21]. Still, however, there is no comprehensive approach available for practical purposes that can simultaneously account for the translational and the rotational component of seismic acceleration, nor has this effect been quantified for structural engineering purposes [22]. This is desirable, especially for bridges supported on cast-in-drilled-hole (single) pile foundations, which are more prone to pile head rotation over pile groups.

Along these lines and with reference to pile–supported bridge piers, the scope of this paper is threefold:

(a) to outline a rational methodology for considering simultaneously the translational and rotational excitation components of a soil–pile–superstructure system,

(b) to present a comprehensive set of parametric analyses and identify cases where the rotational component of the excitation is significant and cannot be neglected,

(c) to provide practical recommendations for incorporating rotational excitation in design.

The analysis framework and the comparative results are presented in the following.

2. DIMENSIONAL ANALYSIS OUTLINE

The study at hand requires the definition of a set of relevant variables that can be grouped into four categories, namely superstructure, CIDH pile foundation, soil, and seismic excitation. The system into consideration, shown in Fig. 1, is a model of a circular bridge pier of diameter d_b and height h_b supporting a deck mass m_b (and J_{mb}), sitting on a single cylindrical pile of diameter d_p with mass m_p (and J_{mp}=0 due to lack of a pile cap) embedded in a uniform soil stratum of shear modulus G_s (i.e., with shear wave velocity $V_s = \sqrt{G_s/\rho_s}$) and thickness H_s. Other important parameters are density and material damping of bridge pier, pile and soil, i.e., $\{\rho_b, \rho_p, \rho_s\}$ and $\{\zeta_b, \zeta_p, \zeta_s\}$, respectively. Both pier and pile are made of reinforced concrete, characterised by the corresponding moduli of elasticity

$\{E_b, E_p\}$. Vertically propagating harmonic S waves of the form $u = u_g e^{i\omega t}$ with bedrock amplitude u_g and circular frequency ω constitute the earthquake excitation. The response parameters of interest are the pier top (deck) displacement due to pure translational and combined translational/rotational excitation, δ_u^{deck} and $\delta_{u+\theta}^{deck}$, respectively, as well as the free field soil response at the ground surface $u_{ff(z=0)}$ being derived from the familiar expression [21]:

$$u_{ff}(z,t) = u_r e^{i\omega t} = u_g \frac{\cos\left(\frac{\omega}{V_s^*} z\right) e^{i\omega t}}{\cos\left(\omega H_s / V_s^*\right)} \tag{1}$$

for depth z=0, where V_s^* $(=\sqrt{G^*/\rho_s})$ is the complex shear wave propagation velocity an $G^* = \sqrt{G_s(1+2\zeta_s)}$ is the corresponding shear modulus. It is recalled that the cyclic natural frequency of the soil $\omega_s = \pi V_s / 2H_s$ and the shear and Young's moduli are related through the expression $G_s = E_s/2(1+\nu)$. Overall, the displacement response of the system δ_u^{deck} depends on 21 independent variables as summarised in Table 1. Note that under linear conditions, the bedrock motion amplitude u_g is not an essential independent variable, as it merely scales the response in proportion to its value. Similarly, the length of the pile L_p does not affect the lateral response at the pile head (assuming long pile conditions), while pier and pile materials are identical, hence, $E_b = E_p$, $\rho_b = \rho_p$ and $\zeta_b = \zeta_p$. Based on the above, the 21+1 characteristic problem variables become 16+1, where 13 are dimensional and 3 (i.e., damping ζ_b, ζ_s and ν) are inherently dimensionless. Accordingly, the response function of the bridge in terms of deck displacement due to translational excitation only, can be written as:

$$\delta_u^{deck} = f(E_b, m_b, J_{mb}, h_b, \rho_b, \zeta_b, d_b, m_p, J_{mp}, d_p, G_s, \nu, H_s, \rho_s, \zeta_s, \omega) \tag{2}$$

The above parameters involve 3 reference dimensions, namely length [L], time [T] and mass [M]. According to Buckingham's theorem, the number of independent dimensionless groups (Π-products) is equal to the number of independent variables reduced by the number of reference dimensions, i.e. 16-3=13 dimensionless groups, hence, one can write:

$$\frac{\delta_u^{deck}}{\delta_{u,ff}^{deck}} = \phi\left(\frac{\omega d_p}{V_s}, \frac{\omega}{\omega_s}, \frac{\omega}{\omega_{bp}}, \frac{E_b}{E_s}, \frac{d_b}{d_p}, \frac{\rho_b}{\rho_s}, \frac{m_b}{m_p}, \frac{J_{mb}}{m_b h_b^2}, \frac{J_{mp}}{m_p d_p^2}, \frac{h_b}{H_s}, \zeta_b, \zeta_s, \nu\right) \tag{3a}$$

Likewise:

$$\frac{\delta_{u+\theta}^{deck}}{\delta_{u,ff}^{deck}} = \phi\left(\frac{\omega d_p}{V_s}, \frac{\omega}{\omega_s}, \frac{\omega}{\omega_{bp}}, \frac{E_b}{E_s}, \frac{d_b}{d_p}, \frac{\rho_b}{\rho_s}, \frac{m_b}{m_p}, \frac{J_{mb}}{m_b h_b^2}, \frac{J_{mp}}{m_p d_p^2}, \frac{h_b}{H_s}, \zeta_b, \zeta_s, \nu\right) \tag{3b}$$

for the case of simultaneous translational and rotational earthquake motion. It is recalled that the first parameter is commonly denoted as normalised frequency $a_0 = \omega d_p / V_s$. The terms:

$$\widehat{I}_u(\omega) = \frac{\delta_u^{deck}}{\delta_{u,ff}^{deck}} \quad \text{and} \quad \widehat{I}_{u+\theta}(\omega) = \frac{\delta_{u+\theta}^{deck}}{\delta_{u,ff}^{deck}} \tag{4}$$

constitute the normalized Engineering Demand Parameters (EDPs) of interest, being herein a form of "modified SSI coefficients" as they express the elastic displacement demand imposed on the bridge pier due to the conventional translation excitation of the pier base and the combined translational/rotational component, respectively, both normalized to the displacement demand of the bridge pier due to the free field displacement at the soil surface. It is recalled to this end, that the above coefficients are analogous to the conventional kinematic interaction coefficients which are defined as [23]:

$$I_u(\omega) = \frac{u_p(\omega)}{u_{ff(z=0)}(\omega)} \tag{5a}$$

$$I_\theta(\omega) = \frac{\theta_p(\omega) d_p}{u_{ff(z=0)}(\omega)} \tag{5b}$$

The dynamic excitation of the bridge is considered in the transverse direction along which the rotational excitation of earthquake ground motion is expected to be more critical due to relatively lower redundancy. A 4–DOF oscillator is adopted, associated with two pairs of translational and rotational DOFs of the two lumped masses (m_b, J_{mb}, m_p and J_{mp}) assumed at the top and bottom of the pier, as shown in Figure 1. A bed of Winkler springs and dampers connecting the pile to the free field soil is used to model soil–pile interaction.

Table 1: Independent problem variables

Variable class	Variable	Units	Fundamental dimensions	Dependence / Significance
Superstructure	Modulus of elasticity, E_b	kN/m²	M,T, L	E_b=E_p
	Mass of superstructure, m_b	t	M	
	Rotational mass of the superstructure J_{mb}	tm²	M, L	
	Pier height, h_b	M	L	
	Pier density, ϱ_b	kg/m³	M, L	ϱ_b= ϱ_p
	Pier material damping, ζ_b	-	-	ζ_b= ζ_p
	Pier diameter, d_b	m	L	
Foundation: R/C CIDH pile	Modulus of elasticity, E_p=E	kN/m²	M,T, L	E_b=E_p
	Mass of foundation, m_p	t	M	
	Rotational mass of the foundation J_{mp}	tm²	M, L	Negligible
	Pile diameter, d_p	M	L	
	Density, ϱ_p	kg/m³	M, L	ϱ_{bp}= ϱ_p
	Material damping, ζ_p	-	-	ζ_{bp}= ζ_p
	Length, L_p	m	L	Irrelevant
Soil	Shear modulus, G_s	kN/m²	M,T, L	
	Stratum thickness, H_s	M	L	
	Density, ϱ_s	kg/m³	M, L	
	Material damping, ζ_s	-	-	
	Poisson's ratio ν	-	-	
Excitation	Cyclic frequency, ω	T	T	
	Bedrock amplitude u_g	m/s²	L,T	Irrelevant

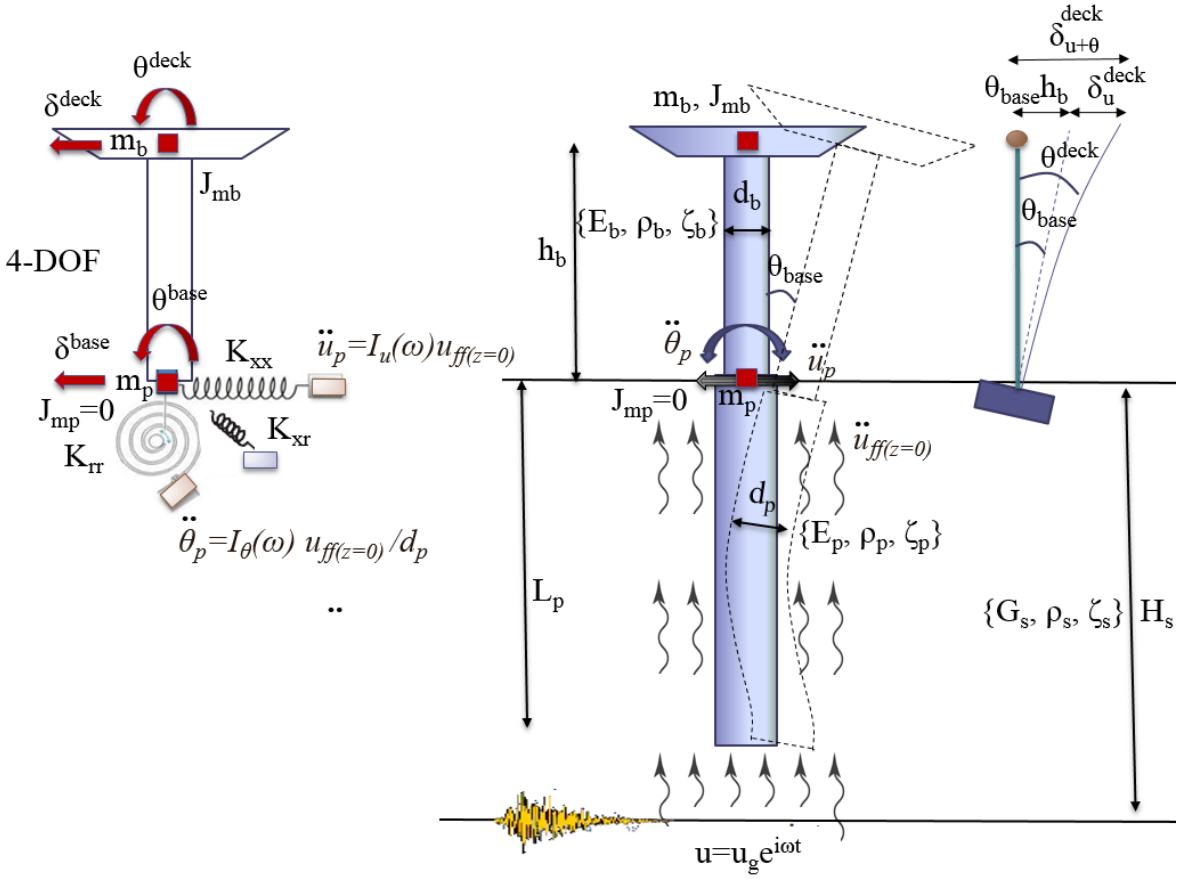

Figure 1: Overview of CIDH pile-bridge system considered and related variables.

3. KINEMATIC AND INERTIAL SOIL-PILE-PIER INTERACTION

3.1 Overview of kinematic and inertial decoupling

The response of bridge–foundation systems, such as the one of Fig. 1, can be computed as the superposition of two effects [24]: (1) the kinematic interaction effect involving the response to base excitation of the actual system assuming zero mass in the superstructure; (2) an inertial interaction effect referring to the response of the complete soil–pile–structure system to excitation by D'Alembert forces associated with the acceleration of the superstructure due to the kinematic interaction. For computational convenience and conceptual simplicity, each one of the above two stages is further subdivided into two independent analysis steps for the needs of this study, as follows:

For the kinematic response: (a_1) analysis of the free–field soil response (i.e. without the presence of piles) to vertically incident *S* waves, $u_{ff}(z,\omega)$ and (a_2) analysis of the interaction of the single pile with the surrounding soil, $u_{pile(z=0)} = I_u(\omega)u_{ff(z=0)}(\omega)$, driven by the free–field response of step (a_1), where z is the depth of the Winkler springs along the pile length and $u_{ff(z=0)}$ the motion at free–field soil surface. To capture in a simple way the rotational component of the excitation, the base rotation exciting the superstructure is derived from the definition of the rotational kinematic response factor, I_θ, eq. (5b):

$$\theta_p(\omega) = \frac{\mathrm{I}_\theta(\omega)u_{ff,z=0}(\omega)}{d_p} \tag{6}$$

For the inertial response: (b_1) computation of the dynamic impedances ("springs" and "dashpots") at the pile head, associated with the swaying $\left(K^*_{xx}\right)$, rocking $\left(K^*_{rr}\right)$ and cross-swaying-rocking $\left(K^*_{xr}\right)$ degrees of freedom at the pile head; and (b_2) analysis of the dynamic response of the superstructure supported on the "springs" and "dashpots" of step (b_1), subjected to the kinematic pile–head motion of step (a_2); the latter consisting the "Foundation Input Motion" (F.I.M.).

The translational $\left(K^*_{xx}\right)$ and rotational $\left(K^*_{rr}\right)$ stiffness of the soil–pile system in step (b1) are derived according to the literature [25] and they are terms of the complex dynamic impedance along any degree of freedom of the system $k^*(z,\omega)$ encompassing the stiffness, inertia, radiation and hysteretic action in the soil, which can be cast in the form:

$$k^*(z,\omega) = k(z,\omega) + i\omega c(z,\omega) \tag{7}$$

Note that no cross–swaying–rocking stiffness term $\left(K_{xr}^{*}\right)$ is employed in the analysis; instead the pier length is increased by a pertinent complex eccentricity e to diagonalise the stiffness matrix, thus uncoupling swaying and rocking response at an extra base node [26]:

$$e = \frac{K_{rx}^{*}}{K_{xx}^{*}} = \frac{1}{2\lambda} \tag{8}$$

where λ is a wave number parameter associated with the attenuation of flexural waves along the pile and z is the vertical coordinate measured from ground surface:

$$\lambda(\omega) = \left[\frac{k_x - m_p\omega^2 + i\omega c_x}{4E_pI_p}\right]^{1/4} \tag{9}$$

with

$$K_{xx}^{*} = 4E_pI_p\lambda^3 \tag{10}$$

$$K_{xr}^{*} = 2E_pI_p\lambda^2 \tag{11}$$

$$K_{rr}^{*} = 2\mathrm{E}_pI_p\lambda \tag{12}$$

$$I_p = \pi d_p^4/64 \tag{13}$$

$$k_x = \delta\cdot\mathrm{E}_s \tag{14}$$

$$c_x(\omega) = (2a_0)^{-1/4}\rho_sV_sd_p\left[1+\left(\frac{V_{La}}{V_s}\right)^{5/4}\right] + 2\frac{\zeta_sk_x}{\omega} \tag{15}$$

k_x, c_x being the corresponding stiffness and damping coefficients, respectively. In the above equations, $V_{La} = {3.4V_s}/{\pi(1-\nu)}$ is a fictitious wave velocity commonly known as "Lysmer's analog velocity" [8, 38]. The dimensionless parameter δ describes spring stiffness and can be approximated as [29]:

$$\delta = 1.67(\mathrm{E}_p/E_s)^{-0.053} \tag{16}$$

The advantage of using the eccentricity transformation in eq. (8) can hardly be overstated, as it greatly simplifies the analysis by avoiding the coupling between rotational and translational response at the base of the model. It is fair to mention that the eccentricity in question is complex valued, resulting

from the damping mismatch between the cross stiffness and horizontal stiffness at the pile head. In this lihght, e should not be viewed as a physical length. From a mathematical viewpoint, this is merely a procedure to diagonalise a matrix [25,26]. An equivalent, yet more complicated approach to handle the cross stiffness term K_{xr} has been proposed by Zania [30]. Also, the use of Lysmer's analog velocity in eq. (15) and the Winkler stiffness δ in eq. (16) are not essential assumptions. Alternatives can be found in a recent study by Karatzia and Mylonakis [31].

3.2 Translational and rotational kinematic interaction

The lateral harmonic deflection $Y(z,t) = Y(z)e^{i\omega t}$, of a vertical elastic pile embedded in a Winkler medium satisfies the well-known equation:

$$\frac{d^4Y(z)}{dz^4} + 4\lambda^4(\omega)\mathrm{Y}(z) = \frac{f(z)}{E_p I_p} \tag{17}$$

where, $f(z)$ are the distributed forces along the pile at each depth z. For earthquake excitation consisting of vertical S waves, the distributed forces along the pile, $f(z)$, is proportional to the free-field horizontal displacements of the soil, u_{ff}, which is determined from one-dimensional wave propagation theory, with boundary conditions of zero shear stresses at the free surface and displacement at the base equal to the induced rock displacement, u_r [21].

Finally, the kinematic response coefficients, $I_u(\omega)$ and $I_\theta(\omega)$ in eq. (5a) and (5b) corresponding to the translational and rotational motion of a free head single pile, are written as [29]:

$$I_u(\omega) = \frac{k + i\omega c}{E_p I_p (q^4 + 4\lambda^4) - m_p\omega^2}\left[1 + \frac{1}{2}\left(\frac{\omega}{V_s\lambda}\right)^2\right] \tag{18}$$

$$I_\theta(\omega) = \frac{k + i\omega c}{E_p I_p (q^4 + 4\lambda^4) - m_p\omega^2}\left(\frac{\omega}{V_s\lambda}\right)^2 d_p\lambda \tag{19}$$

where $q = \omega/V_s$ is the wave number of the vertically–propagating *S* waves. The total excitation of the superstructure (F.I.M.) is a linear combination of the pile head translational motion (i.e. the kinematically altered surface free-field motion), $I_u(\omega)\cdot u_{ff(z=0)}$ and the pile head rotation, θ_p derived from Eq. (6).

3.3 Inertial interaction

The dynamic response of a head-loaded pile has been studied in the literature far more extensively than the corresponding kinematic response to seismic waves. Much of the published work has treated the soil as a continuum and developed numerical and semi-analytical methods to derive the dynamic impedances at pile head. Simple algebraic expressions have also been derived for directly estimating the dynamic impedance of single piles in idealised (homogeneous and inhomogeneous) soil profiles. In this work, use is made of the following solution as derived by Novak [32] and applied in [26]:

$$K_g^* = 2E_p I_p \lambda \begin{bmatrix} 2\lambda^2 & \lambda \\ \lambda & 1 \end{bmatrix} \tag{20}$$

By means of the aforementioned eccentricity transformation, the swaying and rocking stiffness are uncoupled:

$$K_{g,e}^* = \begin{bmatrix} K_{xx}^* & 0 \\ 0 & K_{rr}^* - 2K_{xr}^* e + K_{xx}^* e^2 \end{bmatrix} = 2E_p I_p \lambda \begin{bmatrix} 2\lambda^2 & 0 \\ 0 & 1/2 \end{bmatrix} \tag{21}$$

Note that the eccentricity e is the length of the rigid link introduced in eq. (8), which usually varies between one to three pile diameters depending primarily on $\left(E_p / E_s\right)$ and that the translational stiffness $K_{xx,e}^* = K_{xx}^*$, while $K_{rr,e}^*$ denotes the uncoupled rotational stiffness and is one half the corresponding dynamic rotational stiffness term of the coupled system.

4. DYNAMIC RESPONSE OF THE CIDH PILE-BRIDGE SYSTEM FOR TRANSLATIONAL AND ROTATIONAL EXCITATION

4.1 Time domain solution

Linear-elastic response

Having defined the translational and rotational foundation input motion (F.I.M.) of the system, the response of the bridge deck in terms of total displacements and rotations can be determined by the differential equation of motion in the matrix form of a MDOF system subjected to multiple support excitation [33] while being flexibly supported (Figure 1). In the time domain it can be written as:

$$\begin{bmatrix} M_s & M_c \\ M_c^T & M_g \end{bmatrix} \begin{Bmatrix} \ddot{u}_s(t) \\ \ddot{u}_g(t) \end{Bmatrix} + \begin{bmatrix} C_s & C_c \\ C_c^T & C_{g,e} \end{bmatrix} \begin{Bmatrix} \dot{u}_s(t) \\ \dot{u}_g(t) \end{Bmatrix} + \begin{bmatrix} K_s & K_c \\ K_C^T & K_{g,e} \end{bmatrix} \begin{Bmatrix} u_s(t) \\ u_g(t) \end{Bmatrix} = \begin{Bmatrix} P_s(t) \\ P_g(t) \end{Bmatrix} \tag{22}$$

where:

$$M_s = \begin{bmatrix} m_b & 0 & 0 & 0 \\ 0 & J_{mb} & 0 & 0 \\ 0 & 0 & m_p & 0 \\ 0 & 0 & 0 & J_{mp} \end{bmatrix} \tag{23}$$

is the $n \times n = 4 \times 4$ mass matrix, $n = 4$ being the free (i.e., unconstrained) degrees of freedom, M_g is the $m \times m = 2 \times 2$ zero mass matrix, of the $m = 2$ support degrees of freedom, M_c is the $n \times m$ null coupling mass matrix, $\{u_s(t)\} = \{\delta_{u+\theta}^{deck}(t), \theta_{u+\theta}^{deck}(t), \delta^{base}(t), \theta^{base}(t)\}^{\mathrm{T}}$ is the $n \times 1$ vector of the total displacements corresponding to non-support degrees of freedom (Figure 1), which is written as $\{u_s(t)\} = \{\delta_u^{deck}(t), \theta_u^{deck}(t), \delta^{base}, 0\}^{\mathrm{T}}$ for the case of purely translational excitation, $\{u_g(t)\} = \{u_p(t), \theta_p(t)\}^{\mathrm{T}}$ is the $m \times 1$ vector of the input ground displacements and rotations at the support degrees of freedom, which is essentially the Foundation Input Motion (F.I.M.) in the time domain and is equal to $\{u_g(t)\} = \{u_p(t), 0\}^{\mathrm{T}}$ when the rotational component of excitation is neglected, $\{P_g(t)\}$ is the $m \times 1$ vector of the reaction forces developed at the support degrees of freedom and $\{P_s(t)\} = \{0, 0, 0, 0\}^T$.

Stiffness and damping matrices of the non-support DOFs (K_s and C_s) are defined similarly to the mass terms where as the support DOF stiffness and damping ($K_{g,e}$ and $C_{g,e}$) are derived by eq. (21) by assuming frequency-independent stiffness (which is a reasonable approximation of a CIDH single pile) and damping corresponding to the predominant (mean) frequency f_m of the free-field excitation computed by weighting the amplitudes over a specified range of the Fourier Amplitude Spectrum (FAS) [34]:

$$f_m = 2\pi / \omega_m = \frac{\sum C_i^2}{\sum C_i^2 \frac{1}{f_i}} \tag{24}$$

for 0.25 Hz $\leq f_i \leq$ 20 Hz with $\Delta f \leq$ 0.05 Hz, where C_i are the Fourier amplitude coefficients, f_i are the discrete FFT frequencies between 0.25 and 20 Hz and Δf is the frequency interval used in the FFT

algorithm. Similarly, the kinematic interaction factors required to define the excitation vector $\{u_g(t)\} = \{u_p(t), \theta_p(t)\}^T$ are derived at the mean circular frequency as $I_u(\omega_m)$ and $I_\theta(\omega_m)$.

Therefore, the deck displacements vector is a $(n+m)\times 1 = 6\times 1$ vector, which can be decomposed to a pseudo-static and a dynamic component as follows:

$$\begin{Bmatrix} u_s \\ u_g \end{Bmatrix} = \begin{Bmatrix} u_s^s \\ u_g \end{Bmatrix} + \begin{Bmatrix} u_s^d \\ 0 \end{Bmatrix} \tag{25}$$

where $\{u_s^s\}$ is the $n\times 1 = 4\times 1$ pseudo-static displacements of the non-support DOFs resulting from the solution of the equation of motion ignoring the inertia and damping effects:

$$\begin{bmatrix} K_s & K_c \\ K_c^T & K_{g,e} \end{bmatrix} \begin{Bmatrix} u^t \\ u_g \end{Bmatrix} = \begin{Bmatrix} 0 \\ P_g(t) \end{Bmatrix} \tag{26}$$

and $\{u_s^d\}$ is the corresponding $n\times 1 = 4\times 1$ dynamic displacement vector. It can be shown that eq. 22 can be written with respect to the non-support DOFs only as:

$$[M_s]\{\ddot{u}_s^d\} + [C_s]\{\dot{u}_s^d\} + [K_s]\{u_s^d\} = \{P_g(t)\} = -[M_s][r]\{\ddot{u}_g(t)\} \tag{27}$$

with $\{u_s^s\} = [r]\{u_g\}$, where $[r]$ is an $n\times m = 4x2$ influence coefficient matrix of the ground motion influence on the structure representing the static displacement $\delta_{u+\theta}^{deck}$ and rotation $\theta_{u+\theta}^{deck}$ at the deck level and the respective displacement and rotation at the foundation level $\left(\delta^{base}, \theta^{base}\right)$, that will result when a static unit ground displacement $u_p = 1$ or a static ground rotation $\theta_p = 1$, of the same direction as $\ddot{u}_p$ and $\ddot{\theta}_p$ will be applied to the undeformed (absolutely rigid) model of the structure. In this case:

$$[r] = \begin{bmatrix} 1 & 0 & 1 & 0 \\ -h & 1 & 0 & 1 \end{bmatrix}^T \tag{28}$$

It is noted that eq. 22-28 consist a simpler case of the general multi-support excitation problem, typically met in the case of non-synchronously excited extended structures [35], because the two exciting support degrees of freedom have identical coordinates, extended however to account for dynamic SSI.

By assuming that the damping of the MDoF system is classical, the response of the system for the case of the dual (translational and rotational excitation) can be written in the following form of n decoupled modal equations, where $n=4$ is the number of modes of the system:

$$m_n^*\ddot{q}_n + c_n^*\dot{q}_n + k_n^* q_n = -\sum_{k=1}^{m=2} \varphi_n^T \left[M\right]\{r_k\}\left\{\ddot{u}_{g,k}(t)\right\} \tag{29}$$

where $m_n^* = \varphi_n^T \left[M\right]\varphi_n$ is the modal mass, $k_n^* = \varphi_n^T \left[K\right]\varphi_n = \omega_n^2 m_n^*$ is the modal stiffness, φ_n is the nth eigenvector, $q_n(t)$ is the nth modal coordinate and ω_n is the nth modal frequency of the MDOF system.

The time-history response function of interest can be ultimately written as:

$$\{u(t)\} = \{u_s(t)\} + \{u_d(t)\} = \begin{Bmatrix} \delta_{u+\theta}^{deck}(t) \\ \theta_{u+\theta}^{deck}(t) \\ \delta^{base} \\ \theta^{base} \end{Bmatrix} = \begin{bmatrix} 1 & -h \\ 0 & 1 \\ 1 & 0 \\ 0 & 1 \end{bmatrix} \begin{Bmatrix} u_p(t) \\ \theta_p(t) \end{Bmatrix} + \sum_{k=1}^{m=2}\sum_{i=1}^{n=4} \varphi_i \Gamma_{i,k} D_{i,k}(t) \tag{30}$$

where $\Gamma_{i,k} = \dfrac{L_{i,k}}{M_i} = \dfrac{\varphi_i^T \left[M\right]\{r_k\}}{\varphi_i^T \left[M\right]\varphi_i}$ is the modal participation factor and $D_{i,k}(t)$ is the response of the SDOF oscillator, with the dynamic characteristics of mode i, subjected to the accelerations $\ddot{u}_{g,k}(t)$ of the supports. The above formulation can be used for linear elastic analysis of the system in the time domain for the case of a non-harmonic excitation (i.e., using recorded earthquake ground motions, Section 6.3) with and without the assumption of the rotational component of excitation. The key normalized Engineering Demand Parameters (EDP) of Eq. (4) were then derived as the ratio of the two maxima in time:

$$\hat{I}_u(\omega_m) = \frac{\left|\delta_u^{deck}(t)\right|_{\max}}{\left|\delta_{u,ff}^{deck}(t)\right|_{\max}} \;,\quad \hat{I}_{u+\theta}(\omega_m) = \frac{\left|\delta_{u+\theta}^{deck}(t)\right|_{\max}}{\left|\delta_{u,ff}^{deck}(t)\right|_{\max}} \tag{31}$$

This solution is used in Section 6.3 to derive the elastic displacement demand response history of the system for a set of recorded ground motion excitations.

Non-linear structural response

To assess the non-linear response of the structure, non-linear analyses were performed numerically using a "holistic" finite element model of both the foundation and the superstructure so that the

translational and rotational F.I.M. where inherently considered by the FE model, after appropriate validation against the above solution for the elastic problem. Results were also plotted with the normalized Engineering Demand Parameters (EDP) of eq. (31) versus the normalised frequency a_0 of excitation after appropriate filtering of the transient extremes. This approach is followed in Section 6.4 where the rotational ductility demand of the pier is sought for a set of sinusoidal pulses.

4.2 Frequency domain solution

Given that the problem studied is inherently frequency dependent, the response of the CIDH-pier system is also derived in the frequency domain in order to facilitate the parametric investigation without the simplifying assumptions inevitably made in the time domain formulation. By applying the Fourier Transformation, eq. 27 can also be written in the frequency domain as:

$$\left\{P_{gj}(i\omega)\right\} = \left\{H_j(i\omega)\right\}\left\{U_j(i\omega)\right\} \tag{32}$$

where $\left\{P_g(i\omega)\right\} = -[M_s][r]\left\{\ddot{u}_g(i\omega)\right\}$, $\left\{H_j(i\omega)\right\} = \left(-[M_s]\omega_j^2 + i\omega_j[C_s] + [K_s]\right)^{-1}$ is the frequency response function matrix and $\left\{U_j(i\omega)\right\}$ is the frequency component of the displacement response vector due to the j^{th} frequency of the excitation vector $\left\{P_g(i\omega)\right\}$. It is noted that in this case, the global stiffness matrix of the 4x4 DOF system is also frequency-dependent due to the $K_{xx}(\omega)$ and $K_{rr}(\omega)$ terms of the 2x2 ground support matrix $\left[K_{g,e}\right]$ (eq. 21).

$$[K(\omega)] = \frac{12EI}{h^3}\begin{bmatrix} 1 & h/2 & -1 & h/2 \\ h/2 & h^2/3 & -h/2 & h^2/6 \\ -1 & -h/2 & \left[1+\dfrac{K_{xx}(\omega)h^3}{12EI}\right] & \left[-h/2+K_{xr}(\omega)\right] \\ h/2 & h^2/6 & \left[-h/2+K_{xr}(\omega)\right] & \dfrac{h^2}{3}\left[1+\dfrac{K_{rr}(\omega)h}{4EI}\right] \end{bmatrix}$$

(33)

The same applies to the excitation terms $u_p(\omega) = I_u(\omega)u_{ff(z=0)}$ and $\theta_p(\omega) = I_\theta(\omega)u_{ff(z=0)}/d_p$ which are also frequency-dependent according to equations 5a and 5b. The above solution in the frequency domain has been used for the parametric analysis of Section 5 and 6.2 where the input is harmonic and the structural response linear elastic.

5. CORRELATION OF ROTATIONAL EXCITATION EFFECTS WITH SOIL STIFFNESS & PIER HEIGHT

5.1 Parametric analysis framework

The parametric study was performed considering a reinforced concrete pier resting on a CIDH pile foundation. Parametric analyses explore the variation of the most important problem parameters, namely, soil stiffness (expressed in terms of the shear wave propagation velocity V_s), height of bridge pier h_{bp} and frequency of excitation (i.e., harmonic pulses used in the range 0.5-10Hz at a step of 0.5Hz). Three types of excitation were considered: (a) conventional translation F.I.M., (b) rotational-only excitation and (c) coupled translational/rotational ground motion, leading to a set of 480 analyses (2 soil profiles x 20 frequencies x 4 pier heights x 3 excitation types) as summarised in Table 2. Excitation is considered along the (more critical), transverse direction. Calculations about all analysis steps are implemented computationally through a specifically developed graphical MatLab environment. The results are portrayed in Figures 2 – 9 in two sets. Set A on the left of each figure, shows the normalised Engineering Demand Parameters $\hat{I}_u(\omega)$ and $\hat{I}_{u+\theta}(\omega)$ for conventional (i.e., translational only) and combined (translational and rotational) foundation input motions, respectively, both plotted in terms of dimensionless frequency a_0. Set B on the right illustrates the corresponding relative displacements of the deck ($\delta_{u+\theta}^{deck}$ in Figure 1) which account for both the displacements that are due to pier bending δ_u^{deck} and the rigid body displacements $\theta_p h_b$ due to foundation rotation. It is noted that as the response of the system is linear elastic, there are no plastic rotations θ_{pl} (and subsequent pier top displacements) while the ground movement u_g is also neglected since it does not induce strain on the structure.

5.2 Soft soil (V_s=100m/s)

In Figures 2a to 5a, $\hat{I}_u(\omega)$ and $\hat{I}_{u+\theta}(\omega)$ are plotted for the case of a uniform soil profile with $V_s = 100m/s$ and four different pier heights {20, 12.5, 7.5 and 5m}. For the tallest pier (h=20m), $\hat{I}_{u+\theta}(\omega)$ under combined (translational and rotational) foundation input motion exceeds 10 at specific frequencies (i.e. $\hat{I}_{u+\theta}(\omega) = 14$ at $\omega d_p / V_s = 0.75$), while remaining considerably high for the entire frequency range examined ($0 < \omega d_p / V_s < 1.4$). Clearly, however, this case corresponds to the absolute upper bound of the rotational ground motion excitation influence since:

Case	Excitation		Soil				Pile			Superstructure					
	Type	f (Hz)	V_s (m/s)	E_s (MPa)	ϱ_s (t/m^3)	ζ_s	d_p (m)	L_p (m)	ϱ_p (t/m^3)	h_b (m)	m_b (Mg)	J_{mb} (Mgm^2)	E_b (GPa)	d_b (m)	ζ_b
A	Translational	{0.5,1.0, 1.5,2.0, 2.5,3.0, 3.5,4.0, 4.5,5.0, 5.5,6.0, 6.5,7.0, 7.5,8.0, 8.5,9.0, 9.5,10.0}	100	6.0	1.7	0.07	2	20	2.4	{5.0, 7.5, 12.5, 20.0}	900	14700	29	1.5	0.05
B	Rotational		100	6.0	1.7										
C	Combined		100	6.0	1.7										
D	Translational		250	10.0	1.8										
E	Rotational		250	10.0	1.8										
F	Combined		250	10.0	1.8										

Table 2: Cases of soil–pile–structure systems considered.

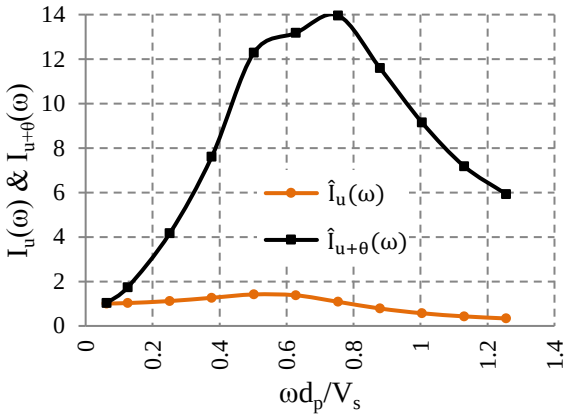

Figure 2a: $\hat{I}_u(\omega)$ and $\hat{I}_{u+\theta}(\omega)$ with a_0 for translational (u) and combined translational-rotational (u+θ) excitation. Soft soil (Vs=100m/s), tall pier (h=20m).

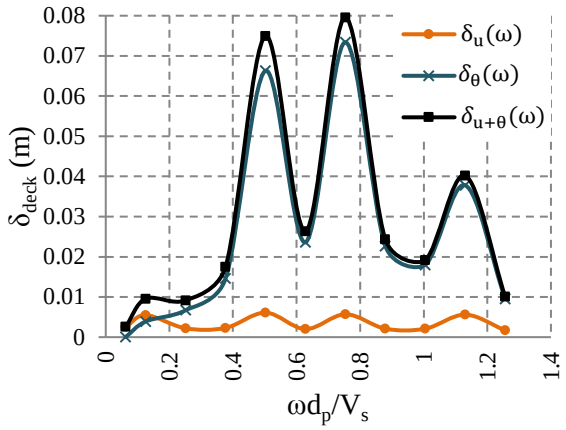

Figure 2b: Deck displacements with a_0 for translational (u) and combined translational-rotational (u+θ) excitation. Soft soil (V_s=100m/s), tall pier (h=20m).

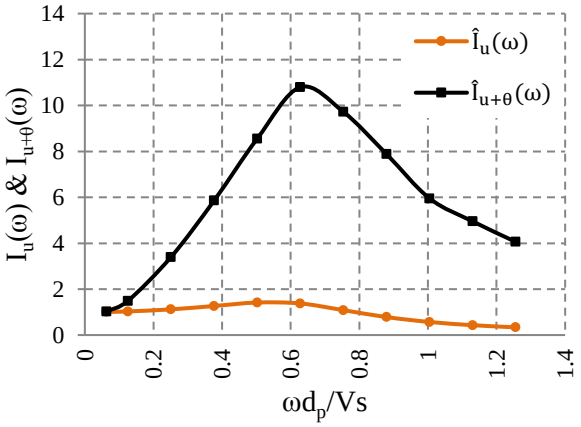

Figure 3a: $\hat{I}_u(\omega)$ and $\hat{I}_{u+\theta}(\omega)$ with a_0 for translational (u) and combined translational-rotational (u+θ) excitation. Soft soil (Vs=100m/s), moderately tall pier (h=12.5m).

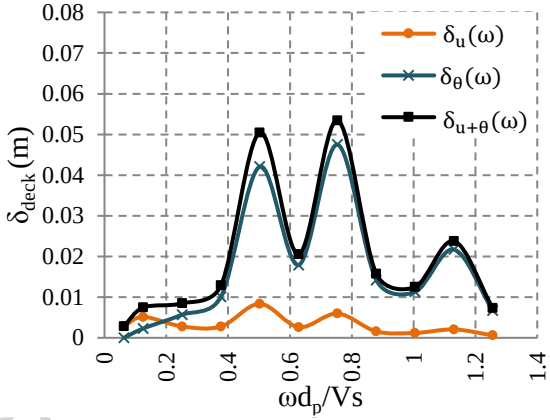

Figure 3b: Deck displacements with a_0 for translational (u) and combined translational-rotational (u+θ) excitation. Soft soil (Vs=100m/s), moderately tall pier (h=12.5m).

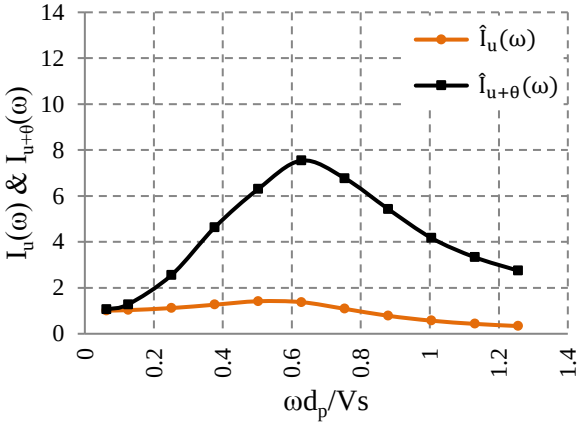

Figure 4a: $\hat{I}_u(\omega)$ and $\hat{I}_{u+\theta}(\omega)$ with a_0 for translational (u) and combined translational-rotational (u+θ) excitation. Soft soil (Vs=100m/s), moderately short pier (h=7.5m).

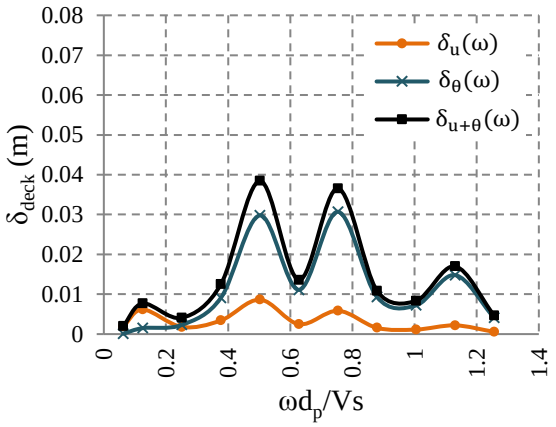

Figure 4b: Deck displacements with a_0 for translational (u) and combined translational-rotational (u+θ) excitation. Soft soil (Vs=100m/s), moderately short pier (h=7.5m).

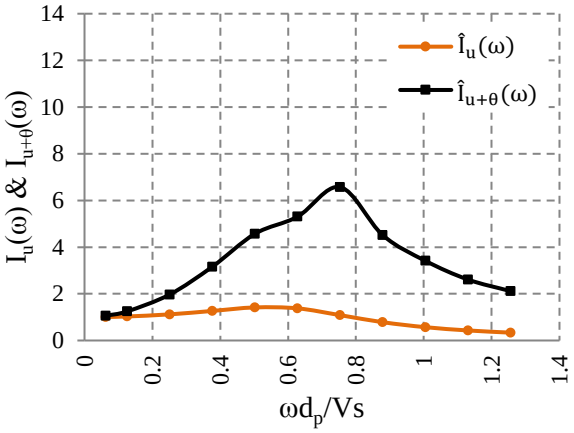

Figure 5a: $\hat{I}_u(\omega)$ and $\hat{I}_{u+\theta}(\omega)$ with a_0 for translational (u) and combined translational-rotational (u+θ) excitation. Soft soil (V_s=100m/s),short pier (h=5.0m).

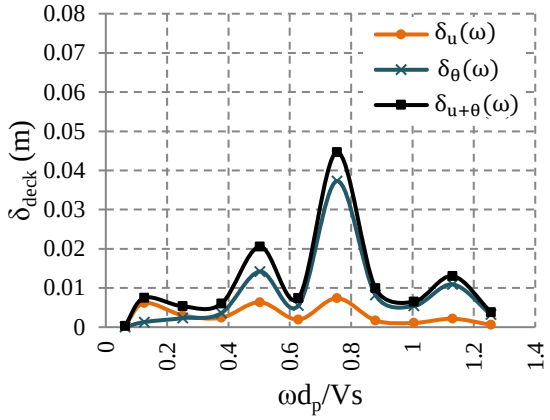

Figure 5b: Deck displacements with a_0 for translational (u) and combined translational-rotational (u+θ) excitation. Soft soil (V_s=100m/s), short pier (h=5.0m).

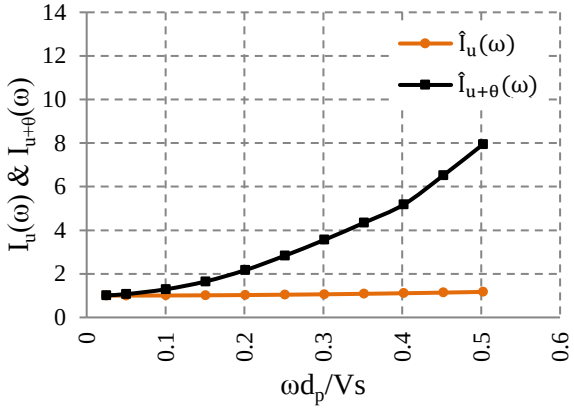

Figure 6a: $\hat{I}_u(\omega)$ and $\hat{I}_{u+\theta}(\omega)$ with a_0 for translational (u) and combined translational-rotational (u+θ) excitation. Moderately stiff soil (V_s=250m/s), tall pier(h=20m).

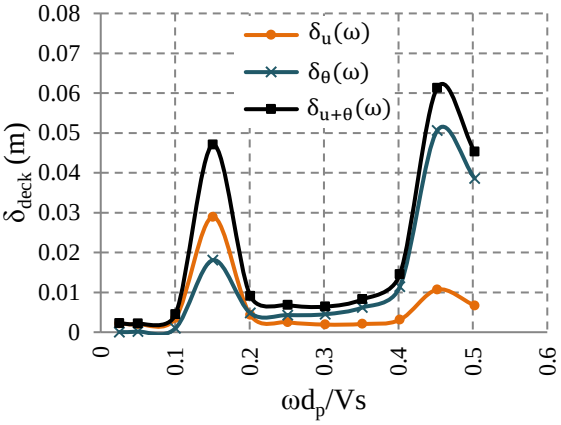

Figure 6b: Deck displacements with a_0 for translational (u) and combined translational-rotational (u+θ) excitation. Moderately stiff soil (V_s=250m/s), tall pier (h=20m).

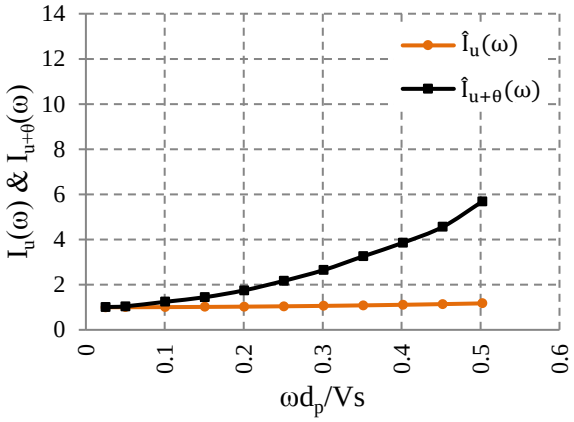

Figure 7a: $\hat{I}_u(\omega)$ and $\hat{I}_{u+\theta}(\omega)$ with a_0 for translational (u) and combined translational-rotational (u+θ) excitation. Moderately stiff soil (V_s=250m/s), moderately tall pier (h=12.5m).

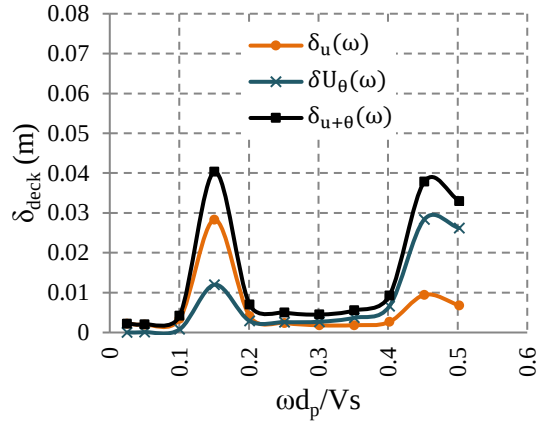

Figure 7b: Deck displacements with a_0 for translational (u) and combined translational-rotational (u+θ) excitation. Moderately stiff soil (V_s=250m/s), moderately tall pier (h=12.5m).

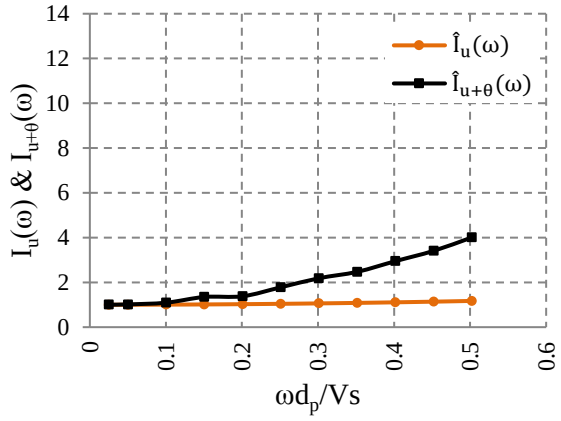

Figure 8a: $\hat{I}_u(\omega)$ and $\hat{I}_{u+\theta}(\omega)$ with a_0 for translational (u) and combined translational-rotational (u+θ) excitation. Moderately stiff soil (V_s=250m/s), moderately short pier (h=7.5m).

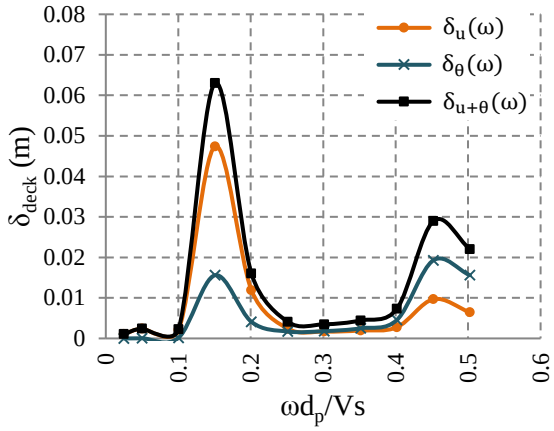

Figure 8b: Deck displacements with a_0 for translational (u) and combined translational-rotational (u+θ) excitation. Moderately stiff soil (V_s=250m/s), moderately short pier (h=7.5m).

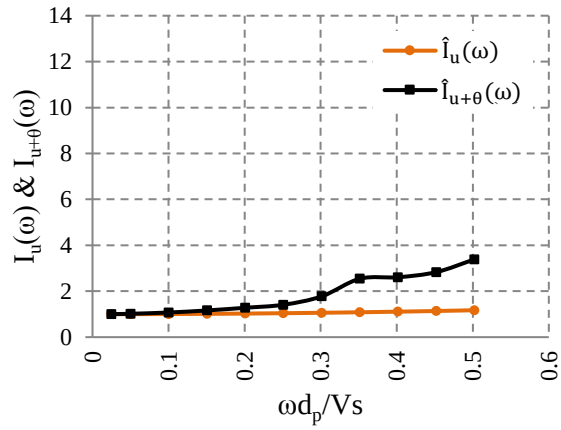

Figure 9a: $\hat{I}_u(\omega)$ and $\hat{I}_{u+\theta}(\omega)$ with a_0 for translational (u) and combined translational-rotational (u+θ) excitation. Moderately stiff soil (V_s=250m/s), short pier (h=5.0m).

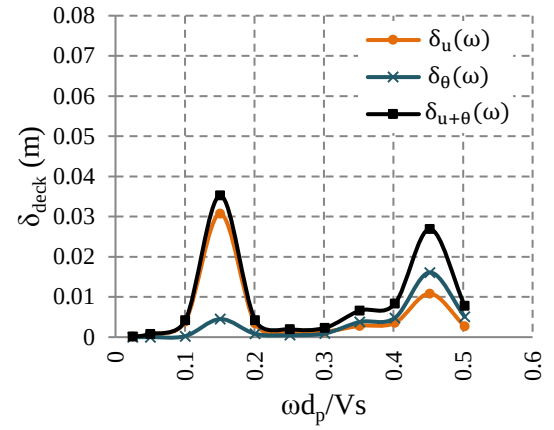

Figure 9b: Deck displacements with a_0 for translational (u) and combined translational-rotational (u+θ) excitation. Moderately stiff soil (V_s=250m/s), short pier (h=5.0m).

(a) soil is very soft (V_s=100m/s), (b) excitation is monochromatic, thus imposing higher seismic demand compared to an actual earthquake motion with a broad frequency content, (c) transverse displacements are sensitive to base rotation since the pier acts as a SDOF system. Furthermore, in very soft soil conditions, pile foundations are designed and a single CIDH pile is a non-compliant solution in most cases. It is interesting however to notice that even for the shorter pier (h=5m), $\hat{I}_{u+\theta}(\omega)$ is reduced to 6.5 but this is still significantly higher compared to the normalised EDP $\hat{I}_u(\omega)$ of the conventional approach, which does not exceed 2 in the entire frequency range.

Similarly, the deck displacements resulting from the combined excitation (translational + rotational), are dominated by the base rotational excitation, as shown in Figures 2b to 5b. Again, the above critical combinations of a soft soil and a harmonic excitation also hold, however, the results illustrate a distinct contribution of the rotational excitation on the displacement demand of the pier, primarily due to the rigid body rotation.

5.3 Soil of moderate stiffness (V_s=250m/s)

Following the same approach, the normalised EDPs and the deck displacements are plotted for the case of moderately stiff soil with V_s=250m/s in Figures 6a-9a and 6b-9b, respectively. The CIDH pile dimensions are kept identical for comparison purposes. Once again, the impact of the rotational excitation of earthquake ground motion on the overall deck displacement demand is evident: the combined response factor $\hat{I}_{u+\theta}(\omega)$ ranges from 3.8 to 8, being always considerably higher than the conventional factor $\hat{I}_u(\omega)$, which does not exceed 1.1 along the entire frequency range examined, for all pier heights.

As anticipated, the effect of the rotational component of foundation input motion, although significant, is lower than the one observed for soft soil, and as such it is expected to be smaller for the case of stiff soil formations (V_s>250m/s). However, the mechanism described previously in which the rotational excitation affects the transverse bridge deck displacements, is again confirmed.

6.0 LINEAR AND NONLINEAR ROTATIONAL EXCITATION EFFECTS ON A CASE STUDY BRIDGE

6.1 Overview of the bridge structure

To further explore the effect of coupled translational and rotational earthquake ground motion excitation on the transverse dynamic response of bridges, a well-studied bridge structure [36] is employed to be studied under both harmonic and transient excitations, in the linear and nonlinear range, respectively. The particular bridge (Figure 10), initially designed with a pile foundation and

redesigned with a CIDH pile to the Eurocodes [3] is a nine-span structure, curved in plan at a radius of 200 m, with a total length of 244 meters. Piers of height varying from 6 to 15 meters are supporting a twin-box girder superstructure with a mass of 3.77 Mg/m and rotational inertia of J_m=15080 Mgm^2. The modulus of elasticity of the reinforced concrete used for both the superstructure and the foundation is E=27.8GPa. The 9m tall, circular pier with a diameter of $d_{bp}=1.5m$ is studied herein, deemed as previously, as a 4-DOF system along the transverse direction. The pier is reinforced with 48Φ32 longitudinal bars, while the transverse reinforcement is Φ12/70mmm for the critical top and bottom 20% of the height and Φ12/140 for the remaining length. The cast-in-drilled-hole pile foundation has a diameter $d_p=2.0m$ and length $L_p=15.0m$ and is embedded in a uniform soil deposit with density and stiffness linearly increasing with depth. For this study, the stratum is considered to be homogenous, characterised by $V_s=360m/s$.

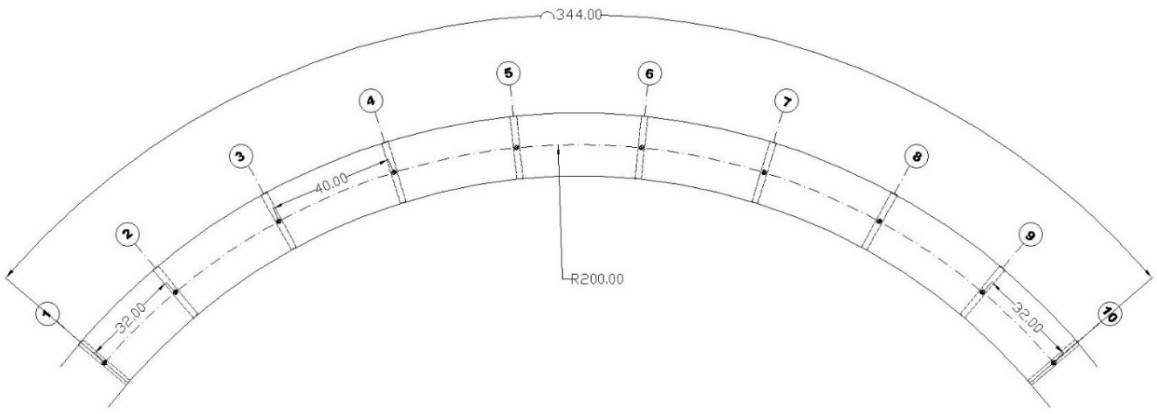

Figure 10: Overview of the bridge plan.

6.2 Elastic displacement demand under harmonic excitation

The results, obtained with the procedure presented in Section 2, are illustrated in Fig. 11a and b portraying the normalised EDPs, $\hat{I}_{u+\theta}(\omega)$ and $\hat{I}_u(\omega)$ (on the left) and the transverse displacements at the deck level (on the right) as a function of the normalised frequency of the excitation $a_0=\omega d_p/V_s$. The natural frequencies of the 4-DOF system are $f_1=0.55Hz$, $f_2=2.29Hz$, $f_3=32.74Hz$ and $f_4=61.72Hz$. It is observed that while the translational-only excitation factor remains practically constant ($\hat{I}_u(\omega)=1.0$, Fig.10a) over the entire frequency range of interest, the combined translational-rotational factor $\hat{I}_{u+\theta}(\omega)$ increases almost proportionally with the dimensionless frequency a_0 for $a_0>0.1$. The maximum value of $\hat{I}_{u+\theta}(\omega)$ is, as anticipated, smaller than the one observed in the case of the moderately stiff soil, due to the higher soil stiffness (V_s=360m/s) and pier height (h=9m). Once more, the triggered rigid body mechanism described

previously significantly contributes to the displacement demand at the pier top leading to up to 2.5 times in relatively high frequencies $a_0 = 0.35$ ($f \approx 10Hz$). It is noted that pier top displacements are amplified at the fundamental frequency of the soil profile $4H_s/V_s = 4 \cdot 15/360 = 6Hz$ ($a_0 \approx 0.20$), as shown in Fig. 11b.

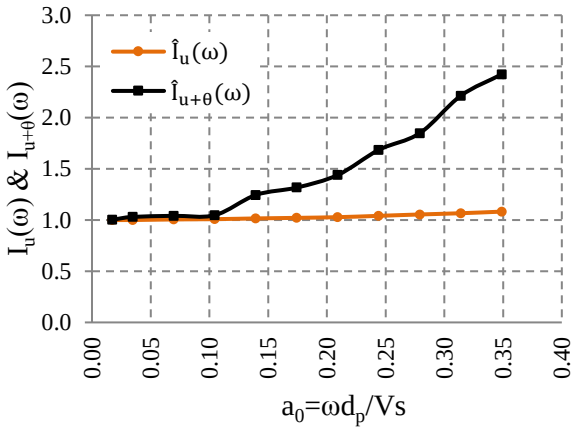

Figure 11a: $\hat{I}_u(\omega)$ and $\hat{I}_{u+\theta}(\omega)$ with a_0 for translational (u) and combined translational-rotational (u+θ) excitation. Stiff soil (V_s=360m/s), pier height h=9m.

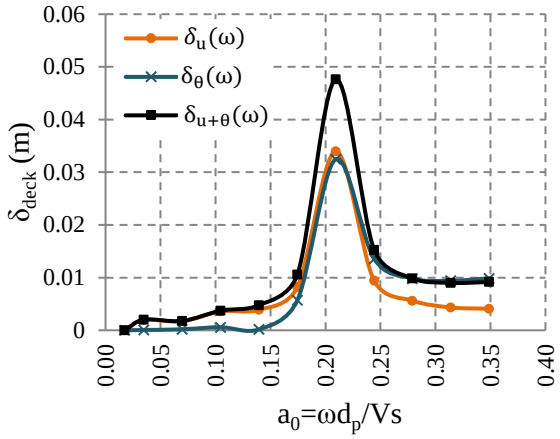

Figure 11b: Deck displacements with a_0 for translational (u) and combined translational-rotational (u+θ) excitation. Stiff soil (V_s=360m/s), pier height h=9m.

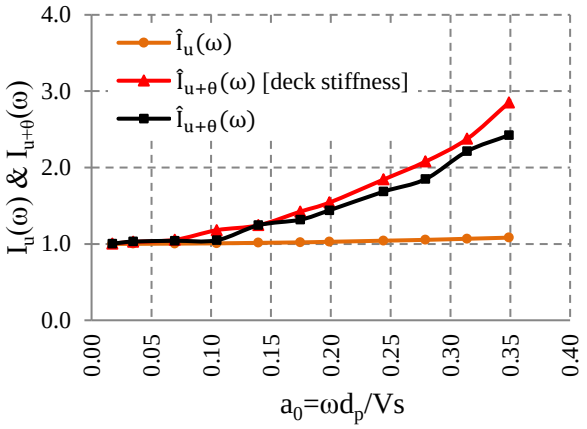

Figure 12a: $\hat{I}_u(\omega)$ and $\hat{I}_{u+\theta}(\omega)$ with a_0 for translational (u) and combined translational-rotational (u+θ) excitation considering deck stiffness. Stiff soil (V_s=360m/s), pier height h=9m.

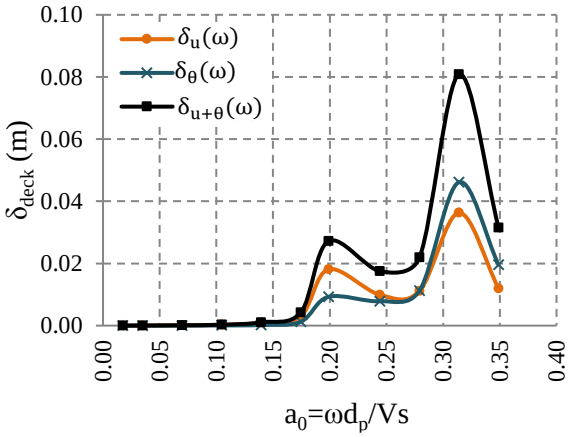

Figure 12b: Deck displacements with a_0 for translational (u) and combined translational-rotational (u+θ) excitation considering deck stiffness. Stiff soil (V_s=360m/s), pier height h=9m.

Influence of deck stiffness

One of the major assumptions made in employing the 4-DOF stick model in the transverse direction is that the bridge is considered adequately long so that the deck does not impose any significant restrain in the transverse movement of the piers. Given that in the case studied, the deck stiffness k_d limits, to some extent, the transverse deformation of the structure and affects the

dynamic characteristics of the system, it was deemed necessary to repeat the analytical procedure considering an additional term associated with the translational DOF of the deck in the stiffness matrix of the 4-DOF system. The deck transverse stiffness k_d was estimated at $3.06 \cdot 10^6 kN/m$ after modelling the entire bridge using the commercial software SAP2000 (ver. 14) [37].

As anticipated, the stiffness of the soil-bridge system was increased, and the first and second natural frequencies were shifted to $f_1 = 1.95Hz$, $f_2 = 9,25Hz$, while f_3 and f_4 remained unaffected. It is notable, however, that the normalised EDP $\hat{I}_{u+\theta}(\omega)$ was found approximately equal or higher to the corresponding one derived for $k_d = 0$ (Fig. 12a). It is also evident that the maximum elastic displacement demand at the pier top along the transverse direction was also shifted to higher frequencies ($a_0 \approx 0.30, f \approx 10Hz$) associated with the (updated) second mode of vibration. Significant displacements are observed for $a_0 \approx 0.20$, which again, correspond to the fundamental frequency of the soil profile. It is concluded that it is important to account for deck stiffness to obtain a more accurate estimate of the seismic displacement along the transverse direction, but the (normalized) effect of rotational excitation of earthquake ground motion remains significant independently of lateral restraint conditions at deck level.

6.3 Elastic displacement demand under transient excitation

Further to the harmonic analysis, a set of 22 accelerograms was selected for studying the transient linear and nonlinear response of the soil-bridge system under purely translational and combined translational-rotational excitations. The ground motions were retrieved by the Pacific Earthquake Engineering Research (PEER) strong motion database [38] using the specialised software ISSARS [39] to cover a broad range of possible earthquake motions with a horizontal peak ground acceleration ranging within 0.16-0.36g. An effort was made to select motions with a breadth of seismological parameters, notably as earthquake magnitude, *M*, source-to-site distance, *R* (both near-and-far field motions were adopted), rupture mechanism and directivity of seismic waves, to keep the frequency content deliberately wide. More precisely, both strong, far-field events (source-to-site distance R>20km, M>6.5) and near-field excitations of moderate intensity (R<20km, magnitude M<6.5) were selected as summarised in Table 3. The small size of the earthquake record sample is due to the deterministic nature of the approach.

The solution (i.e., displacement demand at the pier top) was obtained numerically by modelling the bridge pier - CIDH pile systems as a whole, the latter being laterally supported on vertically distributed springs and dashpots with properties identical to the ones derived analytically (Eq. 14, 15) and attached at an interval of 1m along the pile length. In such a way, kinematic interaction

between the soil and the CIDH pile is inherent in the analysis and the bridge pier is simultaneously subjected to the F.I.M. resulting from translation and rotation of the pile. The purely translational excitation of the bridge pier, required for defining $I_u(\omega)$, was derived by uncoupling the kinematic and inertial interaction and applying solely the translational response of the CIDH pile head as input to the superstructure.

Table 3: Ground motions used in time–domain analyses.

ID	Event	Date	M_w	Station	Source-to-site distance (km)	PGA (g)
1	Whittier Narrows	10/1/1987	5.7	90032 LA-N Figueroa St	11.4	0.166
2	Coalinga	7/22/1983	5.7	1608 Oil Fields Fire Station FF	10.9	0.219
3	Parkfield	28/6/1966	6.1	1438 Temblor pre-1969	9.9	0.357
4	Parkfield	28/6/1966	6.1	1438 Temblor pre-1969	9.9	0.272
5	Coyote Lake	6/8/1979	5.6	57383 Gilroy Array #6	3.1	0.316
6	Morgan Hill	24/4/1984	6.1	57383 Gilroy Array #6	11.8	0.222
7	Morgan Hill	24/4/1984	6.1	57383 Gilroy Array #6	11.8	0.292
8	Palm Springs	8/7/1986	6.0	12149 Desert Hot Springs	8.0	0.331
9	Palm Springs	8/7/1986	6.0	12149 Desert Hot Springs	8.0	0.271
10	Livermore	27/1/1980	5.5	57T02 Morgan Terr Park	8.0	0.198
11	Livermore	27/1/1980	5.5	57T02 Morgan Terr Park	8.0	0.252
12	Loma Prieta	18/10/1989	7.1	1652 Anderson Dam (Downstream)	21.4	0.244
13	Northridge	17/1/1994	6.7	24389 LA-Century City CC North	25.7	0.222
14	Kern County	21/7/1952	7.7	1095 Taft Lincoln School	41	0.178
15	Cape Mendocino	25/4/1992	7.1	89509 Eureka-Myrtle & West	44.6	0.178
16	San Fernando	9/2/1971	6.6	126 Lake Hughes #4	24.2	0.192
17	Landers	6/28/1992	7.4	23559 Barstow	36.1	0.132
18	Imperial Valley	15/10/1979	6.9	6604 Cerro Prieto	26.5	0.169
19	Taiwan	11/14/1986	7.8	29 SMART1 M07	39.0	0.160
20	Superstitn Hills	11/24/1987	6.6	5052 Plaster City	21.0	0.121
21	Northridge	17/1/1994	6.7	24303 LA-Hollywood Stor FF	25.5	0.358
22	Loma Prieta	18/10/1989	7.1	1678 Golden Gate Bridge	85.1	0.233

The normalised EDPs $\hat{I}_u(\omega)$ and $\hat{I}_{u+\theta}(\omega)$ are defined according to Eq. 31 as the ratio of the maximum pier top displacement in time due to purely translational and combined translational-rotational excitation respectively, and the maximum pier top displacement in time due to free field ground motion for both moderate intensity near-field excitations and strong far-field events. The variation with mean normalised frequency $a_{0m} = \omega_m d_p / V_s$ is plotted in Fig. 13, while Table 4 summarises the maximum displacements in time at bridge deck level along with the values of the above normalised factors for each earthquake record.

Several interesting trends are worth noting. *First*, as in the case of harmonic excitation, $\hat{I}_{u+\theta}(\omega)$ is significantly higher (i.e., at least 1.5 times) than $\hat{I}_u(\omega)$ ranging from 2.0 to 4.35. It is also more

sensitive to normalised frequency of excitation as evident by the slope of the fitted line. This indicates that rotational excitation attributed to the bending of the CIDH pile has a non-negligible effect independently of the frequency content of the ground motion than the soil–pile system as a result of the aforementioned rigid body and inertial mechanism.

Secondly, no record exists that is simultaneously the most critical for both types of F.I.M. (i.e., translational or combined translational-rotational excitation). As shown in Table 4, peak value of $\widehat{I}_u(\omega)$=1.77 occurs for the #5 Coyote Lake record, whilst peak $\widehat{I}_{u+\theta}(\omega)$ =4.34 results from the #16 San Fernando motion. While it is the amplitude of ground acceleration that controls the rotational acceleration amplitude, it is also the frequency content of input motion that dominates impact of rotational component of ground motion on the transverse response of the bridge. This is further illustrated by examining the Fourier spectra of the two ground motions that lead to the extreme, higher and lower values of $\widehat{I}_{u+\theta}(\omega)$, in particular of records #16 and #22, respectively. Figure 14 illustrates clearly this relation between the frequency content and the impact of rotational excitation: record #22 is dominated by low frequencies (0<f<2.05Hz), which do not resonate with the dynamic characteristics of the system (f_i>1.95Hz, i=1..4), thus not only minimising the absolute response under translational excitation but also the additional effect of rotational excitation $\widehat{I}_{u+\theta}(\omega)$.

6.4 Rotational ductility demand under sinusoidal pulses

To improve current understanding of the rotational excitation effects on the inelastic seismic performance of the CIDH pile supported bridge studied herein, the rotational ductility demand $\mu_\theta = \left(\theta_{u+\theta}^{deck} - \theta^{base}\right)/\theta_y$ of the system was further explored, where θ_y is the yield rotation of the circular R/C section of the pier. Assuming a steel nominal yield and ultimate strength $f_{yk} = 430MPa$, $f_u = 645MPa$ and characteristic compressive concrete strength $f_{ck} = 35MPa$ for the $d_b = 2.0m$ circular pier section, the yield moment was derived equal to $M_y = 11.3kNm$. The system was again excited with sinusoidal pulses in the time domain ($u = u_g e^{i\omega t}$) within the frequency range 0.5 –10Hz, after applying a scale factor of 3.0 on the bedrock amplitude u_g to illustrate more clearly the impact of rotational excitation in nonlinear regime. Note that both the pile and the soil were considered as linearly visco-elastic.

Table 4: Maximum deck displacements and corresponding EDPs for purely translational and combined translational-rotational (u+θ) excitation. Stiff soil (Vs=360m/s), pier height h=9m.

ID	Event	Station	$\left\|\delta_{u+\theta}^{deck}(t)\right\|_{max}$ (cm)	$\hat{I}_{u+\theta}(\omega)$	$\hat{I}_{u}(\omega)$
1	Whittier Narrows	90032 LA-N Figueroa St	3.26	2,96	1,34
2	Coalinga	1608 Oil Fields Fire Station FF	6.37	3,64	1,53
3	Parkfield	1438 Temblor pre-1969	3.75	2,55	1,14
4	Parkfield	1438 Temblor pre-1969	3.67	3,24	1,18
5	Coyote Lake	57383 Gilroy Array #6	3.84	2,93	1,77
6	Morgan Hill	57383 Gilroy Array #6	7.55	4,17	1,63
7	Morgan Hill	57383 Gilroy Array #6	3.96	2,91	1,34
8	Palm Springs	12149 Desert Hot Springs	7.91	3,96	1,48
9	Palm Springs	12149 Desert Hot Springs	6.75	3,99	1,58
10	Livermore	57T02 Morgan Terr Park	3.34	3,10	1,50
11	Livermore	57T02 Morgan Terr Park	5.22	3,84	1,61
12	Loma Prieta	1652 Anderson Dam (Downstream)	4.04	3,31	1,34
13	Northridge	24389 LA-Century City CC North	3.88	2,71	1,19
14	Kern County	1095 Taft Lincoln School	3.39	3,02	1,40
15	Cape Mendocino	89509 Eureka-Myrtle & West	2.73	2,25	1,14
16	San Fernando	126 Lake Hughes #4	6.47	4,34	1,66
17	Landers	23559 Barstow	1.99	3,79	1,52
18	Imperial Valley	6604 Cerro Prieto	5.58	4,29	1,58
19	Taiwan	29 SMART1 M07	1.33	2,66	1,21
20	Superstitn Hills	5052 Plaster City	2.94	3,37	1,40
21	Northridge	24303 LA-Hollywood Stor FF	9.53	3,56	1,49
22	Loma Prieta	1678 Golden Gate Bridge	2.70	2,10	1,15

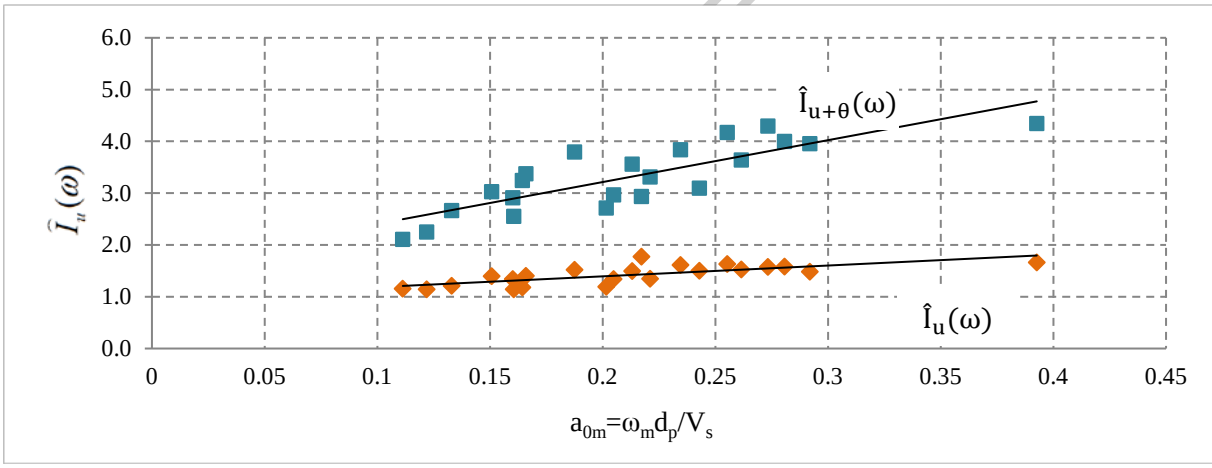

Figure 13: Response influence factor as a function of normalised mean frequency a_{0m} for translational (u) and combined translational/rotational (u+θ) excitation. Stiff soil (V_s=360m/s), pier height h=9m.

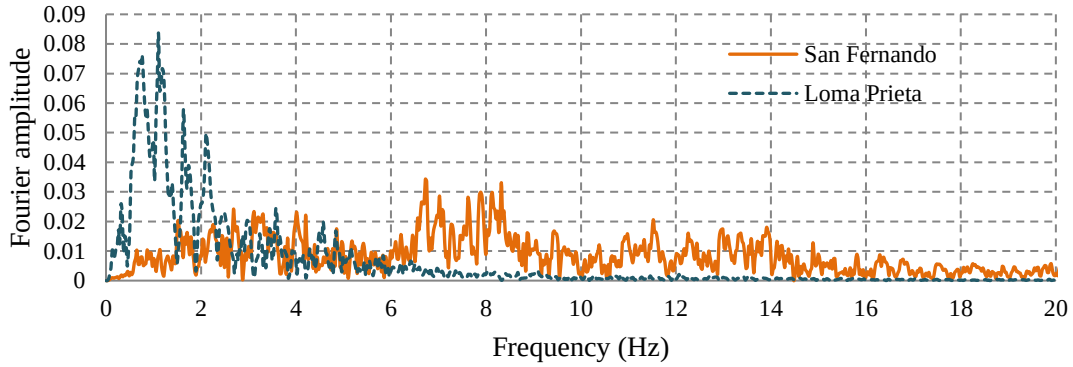

Figure14: Fourier acceleration spectra for extreme (maximum and minimum) factor $\widehat{I}_{u+\theta}(\omega)$. Stiff soil ($V_s$=360m/s), pier height h=9m.

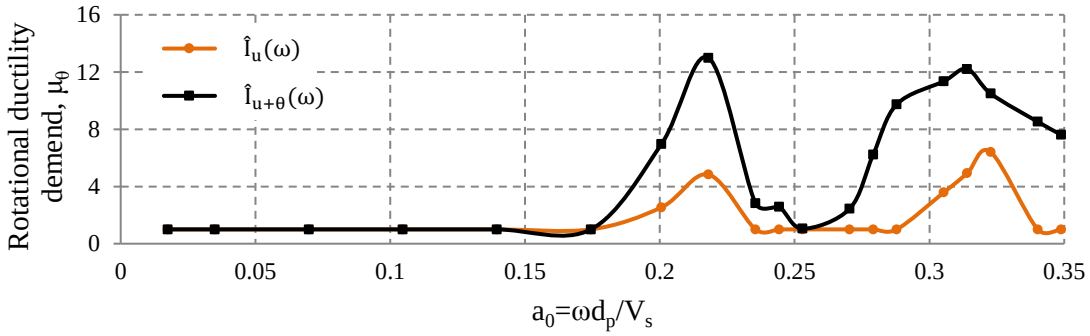

Figure 15: Rotational ductility demand, μ_θ, versus dimensionless frequency for translational (u) and combined translational-rotational (u+θ) excitation. Stiff soil (V_s=360m/s), pier height h=9m.

Figure 15 illustrates the variation of the computed rotational ductility demand, μ_θ, again as a function of normalised frequency a_0. It is shown that in case of translational-only excitation with harmonic pulses, the system remains essentially elastic independently of excitation frequency, except for the characteristic normalised frequencies $\alpha_0 = 0.22$ and $\alpha_0 = 0.32$ where $\mu_\theta = 4.8$ and 6.4., respectively, which coincide with the predominant frequencies of the second mode of vibration of the system and the fundamental period of the subsoil. Combined translational and rotational F.I.M., on the other hand, leads to constantly higher rotational ductility demand which ranges between 1-13 for $\alpha_0 > 0.17$, notably with peaks at the same characteristic normalised frequencies. The above indicate that neglecting the rotational component of earthquake excitation might significantly underestimate the rotational ductility demand imposed on the superstructure, essentially for all ground motions with frequency content in the vicinity of the dynamic properties of the soil-structure system and the subsoil domain.

7. CONCLUSIONS

An analytical and numerical study was presented to quantify the effect of the rotational component of Foundation Input Motion on the elastic and inelastic seismic demand of bridges supported on cast-in-drilled-hole (CIDH) piles in homogeneous soil. It is recalled that such a rotational excitation at the level of the pile head, arises from the bending of single pile during vertical propagation of shear waves and is commonly neglected in design. The study reported herein considers a four-degree-of-freedom spring- and dashpot-supported stick model, representing a bridge pier, subjected to translational-only and combined translational-rotational F.I.M. derived from kinematic interaction analysis. The analytical approach is applied to a set of linear, elastodynamic systems of different height on soft and medium-stiffness soil and is extended for the case of a well-studied bridge subjected to harmonic and actual earthquake records in both the linear and nonlinear range. The main conclusions of the study can be summarised as follows:

The combined translational and rotational seismic input produced by kinematic response of the pile foundation, may substantially amplify (by a factor of more than 1.5), the elastic and inelastic demand of a bridge in the transverse direction, wherein the system is more prone to rigid body rotations compared to the inertial response caused from the translational motion. The amplification, however, is not uniform over the whole frequency spectrum.

The effect of rotational component of seismic input on the dynamic response of the bridge is strongly dependent on pier height, soil stiffness and predominant frequency of earthquake ground motion. Clearly, tall piers resting on soft soils through CIDH pile foundations are more sensitive to rotational excitation effects by a factor 2 to 3. In such cases, a pile group foundation shall be providing a better design, unless the safety factor of the soil-pile system is verified considering the rotational component of ground motion.

It is noted that the proposed analytical approach refers to the linear elastic response of a single, long pile and its surrounding soil, the latter assumed homogenous. Further research is required on quantifying the importance of the rotational excitation for cases of more complex bridge types, foundations and soil conditions.

REFERENCES

[1] Makris N, Gazetas G, Delis E. Dynamic Soil-Pile-Foundation-Structure Interaction: Records and Predictions. Geotechnique 1996;46:33–50.

[2] Sextos AG, Pitilakis KD, Kappos AJAJ, Pitilakis KD. Inelastic dynamic analysis of RC bridges accounting for spatial variability of ground motion, site effects and soil-structure interaction phenomena. Part 2: Parametric study. Earthq Eng Struct Dyn 2003;32:629–52. doi:10.1002/eqe.242.

[3] Kappos AJ, Sextos AG. Effect of foundation type and compliance on seismic response of RC bridges. J Bridg Eng 2001;6. doi:10.1061/(ASCE)1084-0702(2001)6:2(120).
[4] Rovithis E, Pitilakis KD, Mylonakis GE. Seismic analysis of coupled soil-pile-structure systems leading to the definition of a pseudo-natural SSI frequency. Soil Dyn Earthq Eng 2009;29:1005–15. doi:10.1016/j.soildyn.2008.11.005.
[5] Maheshwari B, Truman KZ, El Naggar MH, Gould PL. Three-Dimensional nonlinear analysis for seismic soil–pile-Structure interaction. Soil Dyn Earthq Eng 2004;24:343–56.
[6] Gazetas G. Seismic response of end-bearing single piles. Int J Soil Dyn Earthq Eng 1984;3:82–93. doi:10.1016/0261-7277(84)90003-2.
[7] Makris N, Gazetas G. Dynamic pile-soil-pile interaction. part II: lateral ans seismic response. Earthq Eng Struct Dyn 1992;21:145–62.
[8] Ranf R, Shin H, Eberhard MO, Arduino P, Kramer SL. Experimentally based evaluation of soil-foundation-structure interaction for a reinforced concrete bridge. 8th Natl. Conf. Earthq. Eng. San Fransisco, U.S., 2006.
[9] Chau K, Shen C, Guo X. Nonlinear seismic soil–pile–structure interactions: shaking table tests and fem analyses. Soil Dyn Earthq Eng 2009;29:300–10.
[10] Kamijo N, Saito H, Kusama K, Kontani O, Nigbor R. Seismic tests of a pile-supported structure in liquefiable sand using large-scale blast excitation. Nucl Eng Des 2004;228:367–76.
[11] Bentley KJ, El Naggar MH. Numerical analysis of kinematic response of single piles. Can Geotech J 2000;37:1368–82.
[12] Mylonakis GE, Nikolaou S, Gazetas G, Nikolaou A. Soil-pile-bridge seismic interaction: kinematic and inertial effects. part I: soft soil. Earthq Eng Struct Dyn 1997;26:337–59.
[13] Dezi F, Carbonari S, Leoni G. Kinematic bending moments in pile foundations. Soil Dyn Earthq Eng 2010;30:119–32. doi:10.1016/j.soildyn.2009.10.001.
[14] Mylonakis GE, Gazetas G. Kinematic Pile Response to Vertical P-wave Seismic Excitation. J Geotech Geoenvironmental Eng 2002;128:860–7.
[15] Dezi F, Carbonari S, Leoni G. Static equivalent method for the kinematic interaction analysis of single piles. Soil Dyn Earthq Eng 2010:1–12. doi:10.1016/j.soildyn.2010.02.009.
[16] Nikolaou S, Mylonakis GE, Gazetas G, Tazoh T. Kinematic pile bending during earthquakes: analysis and field measurements. Geotechnique 2001;51:425–440. doi:10.1680/geot.51.5.425.39973.
[17] Manos GC, Pitilakis KD, Sextos AG, Kourtides V, Soulis V, Thauampteh J. Field experiments for monitoring the dynamic soil-structure-foundation response of a bridge-pier model structure at a Test Site. J Struct Eng ASCE 2014:1–11. doi:10.1061/(ASCE)ST.1943-541X.0001154.
[18] Dryden M, Fenves G. The Integration of Experimental and Simulation Data in the Study of Reinforced Concrete Bridge Systems Including Soil-Foundation-Structure Interaction. University of California, Berkeley: 2009.
[19] Sextos AG, Mylona E-KV, Mylonakis GE. A computational framework for the assessment of earthquake-induced rocking in CIDH pile supported bridges. 3rd ECCOMAS Themat. Conf. Comput. Methods Struct. Dyn. Earthq. Eng. (COMPDYN), Corfu, Greece, 2011.
[20] Mylonakis GE, Papastamatiou DY, Psycharis IN, Mahmoud K. Simplified modeling of bridge response on soft soil to nonuniform seismic excitation. J Bridg Eng ASCE 2001;6:587–97.
[21] Roesset JM, Desai CS, Christian JT. Soil amplification in earthquakes. Numerical methods in geotechnical engineering. New York: 1977.
[22] Sextos AG, Mylonakis GE, Mylona E-KV. Rotational excitation of bridges supported on pile groups in soft or liquefiable soil deposits. Comput Struct 2015;155:54–66.
[23] Fan K, Gazetas G, Kaynia AM, Kausel E, Ahmadi E. Kinematic seismic response of single piles and pile groups. J Geotech Eng Div ASCE 1991:1531–48.
[24] Kausel E, Roesset JM. Soil—structure interaction for nuclear containment structures. Power Div. Spec. Conf. Boulder, Colorado: Proc. ASCE; 1994.
[25] Maravas A, Mylonakis GE, Karabalis D. Dynamic characteristics of structures on piles and footings. 4th Int. Conf. Earthq. Geotech. Eng., 2007.
[26] Maravas A, Mylonakis GE, Karabalis DL. Simplified discrete systems for dynamic analysis of structures on footings and piles. Soil Dyn Earthq Eng 2014;61–62:29–39. doi:10.1016/j.soildyn.2014.01.016.
[27] Gazetas G, Dobry R. Simple radiation damping model for piles and footings. J Eng Mech

1984;110:937–56.
[28] Mylonakis GE, Gazetas G. Lateral vibration of internal forces of grouped piles in layered soil. J Geotech Geoenvironmental Eng 1999;125:16–25.
[29] Dobry R, Vicenti E, O'Rourke MJ, Roesset JM. Horizontal stiffness and damping of single piles. J Geotech Eng Div 1982;108:439–59.
[30] Zania V. Natural vibration frequency and damping of slender structures founded on monopiles. Soil Dyn Earthq Eng 2014;59:8–20. doi:10.1016/j.soildyn.2014.01.007.
[31] Karatzia X, Mylonakis GE. Horizontal Stiffness and Damping of Piles in Inhomogeneous Soil. J Geotech Geoenvironmental Eng 2016. doi:10.1061/(ASCE)GT.1943-5606.0001621.
[32] Novak M. Dynamic Stiffness and Damping of Piles. Can Geotech J 1974;11:574–98. doi:10.1139/t74-059.
[33] Clough RW, Penzien J. Dynamics of structures, Third Edition, Computers & Structures, Inc., USA. 2003.
[34] Rathje EM, Faraj F, Russell S, Bray JD. Empirical relationships for frequency ground motions. Earthq Spectra 2004;20:119–44. doi:10.1193/1.1643356.
[35] Sextos AG, Karakostas C, Lekidis V, Papadopoulos S. Multiple support seismic excitation of the Evripos bridge based on free-field and on-structure recordings. Struct Infrastruct Eng 2015;11:1510–23. doi:10.1080/15732479.2014.977302.
[36] Park R. Comparative bridge examples. 2nd Int. Work. Seism. Des. Bridg., New Zealand: 1994, p. Vol.2, 135-145.
[37] CSI. SAP2000: Linear and Nonlinear Static and Dynamic Analysis and Design of Tree-Dimensional Structures 2006.
[38] PEER:NGA database, PEER. Pacific Earthquake Engineering Research. Univ California, Berkeley 2013.
[39] Katsanos EI, Sextos AG. ISSARS: An integrated software environment for structure-specific earthquake ground motion selection. Adv Eng Softw 2013;58:70–85. doi:10.1016/j.advengsoft.2013.01.003.